

# Nonuniversal gaugino masses and seminatural supersymmetry in view of the Higgs boson discovery

Stephen P. Martin

*Department of Physics, Northern Illinois University, DeKalb, Illinois 60115, USA;  
Fermi National Accelerator Laboratory, P.O. Box 500, Batavia, Illinois 60510, USA;  
and Kavli Institute for Theoretical Physics, University of California,  
Santa Barbara, California 93106, USA*

(Received 12 December 2013; published 20 February 2014)

I consider models with nonuniversal gaugino masses at the gauge coupling unification scale, taking into account the Higgs boson discovery. Viable regions of parameter space are mapped and studied in the case of nonuniversality following from an  $F$ -term in a linear combination of singlet and adjoint representations of  $SU(5)$ . I consider, in particular, “seminatural” models that have small  $\mu$ , with gaugino masses dominating the supersymmetry-breaking terms at high energies. Higgsino-like particles are then much lighter than all other superpartners, and the prospects for discovery at the Large Hadron Collider can be extremely challenging.

DOI: 10.1103/PhysRevD.89.035011

PACS numbers: 14.80.Ly

## I. INTRODUCTION

The explorations of the Large Hadron Collider (LHC) at  $\sqrt{s} = 7$  and 8 TeV have significantly impacted the parameter space available for low-energy supersymmetry as a solution to the hierarchy problem. In the once-popular “minimal supergravity” [or “constrained minimal supersymmetric standard model” (CMSSM)] scenario, the lower bounds [1–4] on gluino and up-squark and down-squark masses are now well over 1 TeV in all cases, and are up to about 1.7 TeV in the case that gluino and squark masses are equal. This motivates looking at supersymmetric models that instead have nonuniversal boundary conditions on the soft scalar and gaugino masses. Such models can have lower detection efficiencies through compression of the superpartner mass spectrum. However, the LHC searches still have a significant reach [5–8] even in the limit of a severely compressed superpartner mass spectrum, and for moderate compression, the reach is comparable to that for CMSSM models, for fixed gluino and squark masses.

The increasing lower bounds on superpartner masses appears to require some fine-tuning to accommodate the electroweak scale. (For recent reviews of naturalness in supersymmetry, see Refs. [9–12].) In particular, the supersymmetric Higgs mass parameter  $\mu$  that appears in the Higgs potential has to be balanced against the supersymmetry-breaking Higgs mass parameters, with, including the leading terms from the one-loop effective potential,

$$-\frac{m_Z^2}{2} = |\mu|^2 + m_{H_u}^2 + \frac{3y_t^2}{16\pi^2} \left\{ f(m_{\tilde{t}_1}^2) + f(m_{\tilde{t}_2}^2) - 2f(m_{\tilde{t}}^2) + A_t^2 \frac{f(m_{\tilde{t}_2}^2) - f(m_{\tilde{t}_1}^2)}{m_{\tilde{t}_2}^2 - m_{\tilde{t}_1}^2} \right\} + \dots, \quad (1.1)$$

where terms suppressed by  $1/\tan^2\beta$  or by loop factors are omitted, and  $f(x) = x \ln(x/Q^2) - x$ , with  $Q$  the renormalization scale at which all of the other parameters on the right side are evaluated as running parameters. Also,  $A_t = a_t/y_t$ , where  $a_t(H_u^+ \tilde{b}_L - H_u^0 \tilde{t}_L) \tilde{t}_R^*$  appears in the soft supersymmetry-breaking Lagrangian.

Increasing bounds on superpartner masses do not imply fine-tuning of  $\mu$  by itself. This is because  $\mu$  is multiplicatively renormalized, and can be obtained from dimensionless supersymmetry-preserving couplings (which can be small, completely naturally) multiplied by supersymmetry-breaking parameters, as in either the Kim-Nilles [13] or Giudice-Masiero [14] mechanisms or the next-to-minimal supersymmetric standard model [15], for example. However, in order to accommodate the known small value of  $-m_Z^2/2$ , it appears to be necessary to “tune” the remaining terms on the right side of Eq. (1.1) against  $|\mu|^2$ . This has led to the popularity of the ideal of “natural supersymmetry” (see e.g. Ref. [16]), in which one argues that therefore  $|\mu|$  should be not more than a few hundred GeV, and that top-squark masses (and the gluino mass, which feeds into them through radiative corrections) should be not much heavier, perhaps below a TeV or so. Because there is no objective measure on parameter space, it is not possible to be more precise than this using unambiguous scientific arguments.

This “natural supersymmetry” parameter space has not yet been eliminated by LHC direct searches for the gluino, top squarks, and Higgsinos, but it is increasingly under tension (see, for example, [17]). Furthermore, the measured Higgs mass is difficult to obtain if both top squarks are light. Therefore one might retreat to a more limited notion that I will refer to as “seminatural supersymmetry,” in which only  $|\mu|^2$  is required to be small (say, less than a few hundred GeV). This can be viewed as requiring only one tuning; namely, the rest of the right-hand side of Eq. (1.1).

This tuning is simply accepted, as it is preferable to the qualitatively more ridiculous tuning associated with non-supersymmetric extensions of the Standard Model. From this perspective, there is no real problem with the observed Higgs boson mass, since one does not require top squarks to be light. The same sort of idea has been considered under the name “Higgsino lightest supersymmetric particle (LSP) world” in [18–20], and the phenomenology has been studied in depth in [20] (see also [21]) for a realization that is qualitatively similar but somewhat different from the present paper. The “focus-point” scenario [22–27] at large scalar masses is another well-known example realizing small  $\mu$ .

In CMSSM models, the largest contributions to  $m_{H_u}^2$  at the electroweak scale are due to the influence of the gluino mass through renormalization group running [28,29]. It has long been appreciated and studied [28–54] that if one abandons the usual CMSSM boundary condition of equal gaugino masses at the scale of apparent unification of gauge couplings, then the little hierarchy problem can be ameliorated. Specifically, this can be accomplished by choosing the gluino mass parameter ( $M_3$ ) to be smaller than the wino mass parameter ( $M_2$ ) by a factor of roughly 3 at the scale of the apparent unification of gauge couplings,  $M_U$ . This leads to smaller values of  $|\mu|^2$ , which is taken here as an indirect indicator for seminatural supersymmetry, as explained above. There are many ways to achieve this, including the possibility [55–61] that the  $F$ -term that breaks supersymmetry and gives mass to the gauginos is not in a pure singlet representation of the global  $SU(5)$  or larger group that contains the Standard Model gauge group  $SU(3)_C \times SU(2)_L \times U(1)_Y$ . These models were the subject of much study even before the LHC turned on, in part because the supersymmetric little hierarchy problem was evident already with the negative Higgs search results of the LEP2 collider.

Reference [41] contained a study of this possibility and showed the existence of regions of parameter space that feature much less extreme cancellation between  $|\mu|^2$  and the rest of Eq. (1.1) than can be found in CMSSM for the same gluino and squark mass scales. In particular, regions of parameter space were exhibited that obtain small values of  $|\mu|$ , similar to the focus-point case and continuously connected to it in parameter space, but with the superpartners as light as could be tolerated by the direct search limits at the time. However, this paper appeared just before the discovery [62–65] of the Higgs boson with a mass near 126 GeV. As a consequence, almost all of the interesting parameter space chosen in [41] is now apparently ruled out by the Higgs boson mass. The purpose of the present paper is to present a similar study, but now updated to include consistency with the Higgs discovery. Here, one should take into account the very significant uncertainties in the theoretical prediction of the Higgs mass [66–107]. As emphasized in [107], it is likely that the leading  $\mathcal{O}(\alpha_s^2 y_t^2)$

three-loop corrections not used in most publicly available two-loop programs [94]–[105] and calculations, but appearing in [92,93], and the public three-loop program H3m [106], will raise the Higgs mass prediction significantly, especially for very large top-squark masses. However, there is an effect from the three-loop  $\mathcal{O}(\alpha_s y_t^4)$  contributions [92] which appears to dilute this effect by perhaps half. In my opinion, this situation really just highlights the theoretical uncertainties that are still large in the case of one or both top squarks very heavy, despite the great efforts that have gone into calculating multiloop corrections. In the following, I will simply use the MSSM model program SuSpect [100] to translate parameters into physical masses, but then allow the predicted value of  $M_h$  to fall anywhere in the region from 123 to 128 GeV.

In any study of MSSM parameter space, somewhat arbitrary choices must be made in order to keep the presentation finite. (See however [108–110].) Below, I will choose to consider only modifications of the CMSSM in which the gaugino mass parameters are nonuniversal in such a way as would follow from  $F$ -terms in a mixture of a singlet and a **24** representation of  $SU(5)$ , following Ref. [41]. The gaugino masses are parametrized at  $M_U$  as

$$M_1 = m_{1/2}(c_{24} + s_{24}), \quad (1.2)$$

$$M_2 = m_{1/2}(c_{24} + 3s_{24}), \quad (1.3)$$

$$M_3 = m_{1/2}(c_{24} - 2s_{24}), \quad (1.4)$$

where  $m_{1/2}$  is an overall gaugino mass scale, and  $c_{24} = \cos \theta_{24}$  and  $s_{24} = \sin \theta_{24}$ , where  $\theta_{24}$  is an angle that parametrizes how much of the  $F$ -term is in the adjoint representation of  $SU(5)$ . In particular,  $\theta_{24} = 0$  is the usual CMSSM-like unified gaugino mass case, while  $\theta_{24} = \pm\pi/2$  is the case of a pure **24** of  $SU(5)$ . Shifting  $\theta_{24}$  by  $\pi$  corresponds to changing the signs of all three gaugino masses, which is the same as changing the signs of the scalar cubic couplings and the  $\mu$ -term. In the following, I will consider slices of parameter space with fixed  $M_3$ , as this corresponds to roughly constant values of the physical gluino mass, often the most important figure of merit for present LHC bounds. The sign of  $\mu/M_3$  will be taken positive. For simplicity, I will also follow [41] by keeping the scalar masses universal at  $M_U$ , parametrized by a variable  $m_0$  as in the CMSSM. Then, as shown in [41], the parameter space that evades direct constraints on superpartners splits into disjoint “continents” (and some small islands) when mapped in the  $m_0$  vs  $\theta_{24}$  plane. The “oceans” between the continents (where no viable solutions occur) include the cases where  $\theta_{24}/\pi \approx -0.102$  where  $M_2/M_3$  approaches 0, and  $\theta_{24}/\pi \approx 0.148$  where  $M_1/M_3$  and  $M_2/M_3$  become very large, and  $\theta_{24}/\pi \approx -0.25$  and  $0.75$  where  $M_1/M_3$  approaches 0. Unlike [41], I will also consider cases of large scalar cubic couplings, as this

facilitates larger  $M_h$  for fixed values of the other parameters. The most straightforward way of evading the LHC bounds on superpartner masses is to simply take the gluino mass parameter  $M_3$  to be large enough so that the gluino and up and down squarks are heavier than 1.7 TeV.

In the following, I will map out the predicted values of the  $\mu$  parameter for several parameter space planes, showing how small  $\mu$  can naturally be obtained outside of the usual focus-point region. This includes regions of parameter space in which soft supersymmetry breaking is dominated by large gaugino masses, with  $m_{1/2}^2$  exceeding  $m_0^2$  and  $A_0^2$  by orders of magnitude. By doing this, one finds that constraints from flavor-violating processes such as  $b \rightarrow s\gamma$  and  $B_s \rightarrow \mu^+\mu^-$  are easily evaded throughout the parameter spaces considered below. The contribution to the muon anomalous magnetic moment is no worse (and not significantly better) than in the Standard Model. I will require that the LSP is a neutralino, and also map out regions of parameter space according to the predicted relic density of dark matter (obtained using the program micrOmegas [111–114]). Here it is important to realize that even if the prediction is far off from the current value of  $\Omega_{\text{DM}}h^2 = 0.12$  from [121,122], the model can still be viable. If the prediction for  $\Omega_{\text{DM}}h^2$  is too low, then axions or something else could be part or all of the dark matter. If the prediction for  $\Omega_{\text{DM}}h^2$  is too high, then the lightest neutralino  $\tilde{N}_1$  could decay, either by  $R$ -parity violation, or into some lighter  $R$ -parity odd particle  $\chi$ , which would reduce  $\Omega_{\text{DM}}h^2$  by a factor of  $M_\chi/M_{\tilde{N}_1}$  [115–118]. Nevertheless, it is interesting to consider the simplest case in which  $\tilde{N}_1$  is assumed to be stable with a thermal relic abundance. I will use the term "allowed neutralino dark matter" (DM) for the case that the predicted thermal  $\Omega_{\text{DM}}h^2 < 0.12$ , where either  $\tilde{N}_1$  is the dark matter or a subdominant component of it, no matter how small. The complementary region where  $\Omega_{\text{DM}}h^2 > 0.12$  will also be mapped, and the boundary between these two regions is where one can straightforwardly take  $\tilde{N}_1$  to be the dominant dark matter component with a thermal relic abundance. Here, it will turn out that much of the parameter space is consistent with the recent XENON100 [119] and LUX [120] direct detection constraints.

## II. MODELS WITH SMALL STOP MIXING ( $A_0 = 0$ )

First, consider a class of models that is of interest because it includes, as a special case, the choice that was used by the LHC experimental collaborations to constrain CMSSM models with early data at  $\sqrt{s} = 7$  and 8 TeV. Take  $\tan\beta = 10$ ,  $\mu > 0$ , and  $A_0 = 0$  in the usual CMSSM language, and allow  $m_0$  and  $\theta_{24}$  to vary. Maps of the resulting parameter space for  $\mu$  and for  $\Omega_{\text{DM}}h^2$  are shown in Fig. 1 for the case of  $M_3 = 2000$  GeV at  $M_U$ . The allowed parameter space is divided into three distinct continents. As explained in [41], the range for the plots is chosen to be  $-1/4 < \theta_{24}/\pi < 3/4$  in order to avoid splitting

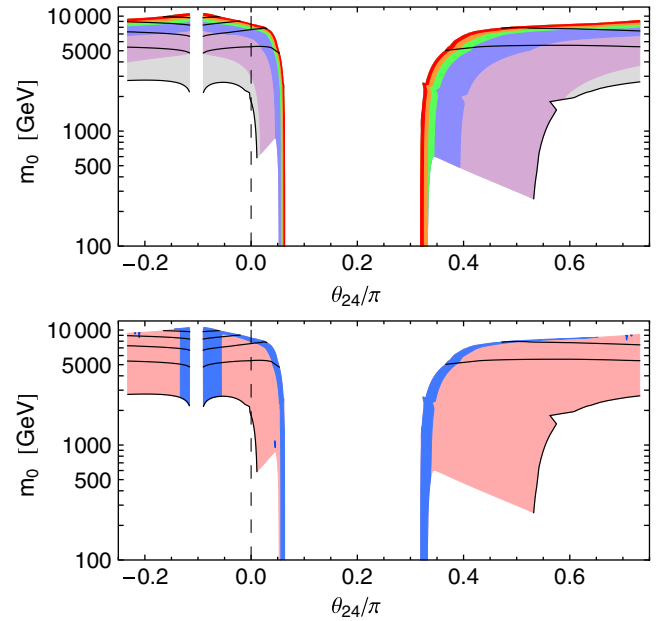


FIG. 1 (color online). Maps of the  $\mu$  parameter (top) and  $\Omega_{\text{DM}}h^2$  (bottom), in the  $m_0$  vs  $\theta_{24}/\pi$  plane, for fixed  $\tan\beta = 10$ , and  $A_0 = 0$ ,  $M_3 = 2000$  GeV at  $M_U$ . The vertical dashed line at  $\theta_{24} = 0$  is the special case of the CMSSM. In each region, the lowest black solid line corresponds to  $M_h = 123$  GeV as calculated by SuSpect, with each higher black line having  $M_h$  increased by 1 GeV. In the top figure, the different shaded regions from top to bottom correspond to  $\mu < 500$ , 750, 1000, 1500 and 2000 GeV, with the lowest (gray) shaded region for  $\mu > 2000$  GeV. In the lower figure,  $\Omega_{\text{DM}}h^2 < 0.12$  is darker shaded and  $\Omega_{\text{DM}}h^2 > 0.12$  is lighter shaded. The same color conventions will be used throughout this paper.

up the continents unnaturally on the map. The vertical dashed line at  $\theta_{24} = 0$  represents the special case of CMSSM on this plot and similar ones below.

In Fig. 1(a), and similar figures below, the different shaded regions correspond to different values of  $\mu$ , according to:

$$\mu < 500 \text{ GeV,}$$

$$500 \text{ GeV} < \mu < 750 \text{ GeV,}$$

$$750 \text{ GeV} < \mu < 1000 \text{ GeV,}$$

$$1000 \text{ GeV} < \mu < 1500 \text{ GeV,}$$

$$1500 \text{ GeV} < \mu < 2000 \text{ GeV,}$$

$$\mu > 2000 \text{ GeV}$$

(from top to bottom).

The lowest black line on each continent shows where SuSpect predicts  $M_h = 123$  GeV, with each higher line corresponding to 1 GeV larger for the  $M_h$  prediction. Recall that the theoretical uncertainties are such that predicted values of 123 GeV may well be consistent with the observed Higgs mass. (Boundaries of the shaded region that are not black solid lines correspond to the requirements of a neutral LSP, no charged superpartner less than



100 GeV accessible to LEP searches, or correct electroweak symmetry breaking.) An important feature of this parameter space is that as  $\theta_{24}$  increases from 0, the region compatible with the observed Higgs mass increases, extending down to lower values of the scalar masses as parametrized here by  $m_0$ . This is because of the relatively larger top-squark mixing.

In each of the continents in Fig. 1(b), the region with  $\Omega_{\text{DM}} h^2 < 0.12$  is shown in darker shaded, and the region with  $\Omega_{\text{DM}} h^2 > 0.12$  is in lighter shaded. The boundary between these two shaded regions agrees with the cosmological results from the WMAP [121] and Planck [122] experiments. Several regions can be seen in Fig. 1(b) to have allowed neutralino dark matter. In the CMSSM case ( $\theta_{24} = 0$ ), the focus-point region [22–27] occurs at  $m_0 \approx 7900$  GeV. As one moves to larger values of  $\theta_{24}$ , this region with allowed neutralino dark matter and small  $\mu$  moves to much lower values of  $m_0$ , until for  $\theta_{24}/\pi$  near 0.056 it extends down to very small  $m_0$ . The plot is cut off at  $m_0 = 100$  GeV for artistic reasons, but in fact the allowed region even extends down to negative  $m_0^2$ . Unlike the situation in the CMSSM, this is possible because the LSP is a Higgsino-like neutralino here, rather than a charged slepton, due to the small value of  $\mu$ , as can be seen in Fig. 1(a). It is interesting that the parameter space thus allows gaugino mass domination of the soft terms, consistent with the constraints of proper electroweak symmetry breaking,  $M_h$ , and allowed neutralino dark matter, and providing a solution of the supersymmetric flavor problem similar to “no-scale” [123–125] or “gaugino mediated” [126–128] models.

On the other side of the CMSSM-like continent in Fig. 1, with  $\theta_{24} < 0$ , the focus-point region occurs at larger values of  $m_0$ . On the left side of this continent, on a vertical line with  $\theta_{24}/\pi \approx -0.056$ , there is sufficient wino mixing in the LSP to give efficient dark matter coannihilation [129–132]. This corresponds to a mostly bino LSP with winos that are only 30 GeV or so heavier. In the corner of parameter space with large  $m_0 \sim 10$  TeV and  $\theta_{24}/\pi \approx -0.056$ , the focus-point and small  $M_2$  regions merge in a realization of the “well-tempered neutralino” [133] with  $\mu$  and  $M_2$  both comparable to  $M_1$ , so that the LSP is a mixture of bino, wino, and Higgsino in the right proportions to allow efficient annihilation of dark matter in the early universe.

In the rightmost continent in Fig. 1, extending from  $0.33 < \theta_{24}/\pi < 0.72$ , there is likewise a focus-point-like region with large  $m_0$ . This region is again continuously connected to a small- $\mu$  region, here along the continent’s left edge at  $\theta_{24}/\pi \approx 0.33$ . This small- $\mu$  region once again extends down to negligibly small  $m_0$ , with gaugino mass dominance giving a solution to the supersymmetric flavor problem, and small values of  $\mu$  providing seminatural supersymmetry.

On the leftmost continent, with  $-0.232 < \theta_{24}/\pi < -0.116$ , there is still a very thin focus-point region with

small  $\mu$  at large  $m_0$ , but this does not connect to any regions with small  $m_0$ . In both the leftmost and rightmost continents, there are small regions at very large  $m_0$  in which allowed neutralino dark matter is achieved through near-resonant binolike LSP annihilation through  $s$ -channel  $Z$  and  $h$  exchange [134]. These small regions, with  $m_{\tilde{N}_1}$  near  $M_Z/2$  and  $M_h/2$  respectively, are centered near  $\theta_{24}/\pi = -0.219, 0.716$  and near  $-0.211, 0.707$  respectively. In these models, the only superpartners that are kinematically accessible to the LHC besides the binolike LSP are the Higgsino-like  $\tilde{N}_2, \tilde{N}_3$  and  $\tilde{C}_1$  with typical masses of several hundred GeV.

The existence of the separate continents as seen in Fig. 1 is a generic feature of the parameter space of models described by a mixture of  $SU(5)$  singlet and adjoint  $F$ -term gaugino masses. However, for simplicity, in the remainder of this paper I will restrict attention to the CMSSM-like continent that is continuously connected to  $\theta_{24} = 0$ .

The maps of the  $\mu$  parameter and allowed neutralino dark matter, for models consistent with  $M_h$  and other constraints, are shown in Fig. 2 for  $M_3 = 1200, 1500, 2000$ , and 2500 GeV. In each case,  $A_0 = 0$ , and  $\tan\beta = 10$ , with  $\mu > 0$ , just as in Fig. 1. The  $M_3 = 1200$  case was chosen as this is one of the lowest values for which  $M_h$  is consistent with observation in an appreciable region of parameter space, although one must have  $m_0 \gtrsim 5000$  GeV. The reason that significantly lower  $M_3$  will not work with these parameters is that to try to accommodate  $M_h$  one must increase the scalar masses (through  $m_0$ ) so much that electroweak symmetry breaking does not work (the solution for  $|\mu|^2$  from the effective potential becomes negative).

For both  $M_3 = 1200$  and 1500 GeV, the resulting allowed neutralino dark matter region in Fig. 2 consists of a focus-point region with small  $\mu$  that is continuously connected to a region on the left (with  $\theta_{24}/\pi \lesssim -0.055$ ) where  $M_2$  is smaller, giving a binolike neutralino LSP with significant wino content. For  $M_3 = 1500$  GeV, this region extends to slightly smaller values of  $m_0$ , but one must still have  $m_0$  larger than 4000 GeV.

For larger  $M_3$ , the region consistent with  $M_h$  in Fig. 2 increases dramatically. As noted above, for  $M_3 = 2000$  GeV and  $M_3 = 2500$  GeV, the region of allowed neutralino dark matter then extends to very small values of  $m_0$  on the right side of the continent, with  $\theta_{24}/\pi \gtrsim 0.05$ . (Note that the  $M_3 = 2000$  GeV case is just a close-up of the full map shown in Fig. 1.) In particular, for  $\theta_{24} > 0$ , the viable region where  $M_h$  is large enough is seen to include much lower values of  $m_0$  than in CMSSM, and even extends down to  $m_0^2 < 0$ . This also coincides with a region of allowed neutralino dark matter with small  $\mu$ . This region is continuously connected to the focus-point region. The region is particularly attractive because the gaugino mass dominance provides a natural solution to the supersymmetric flavor problem; flavor violation is

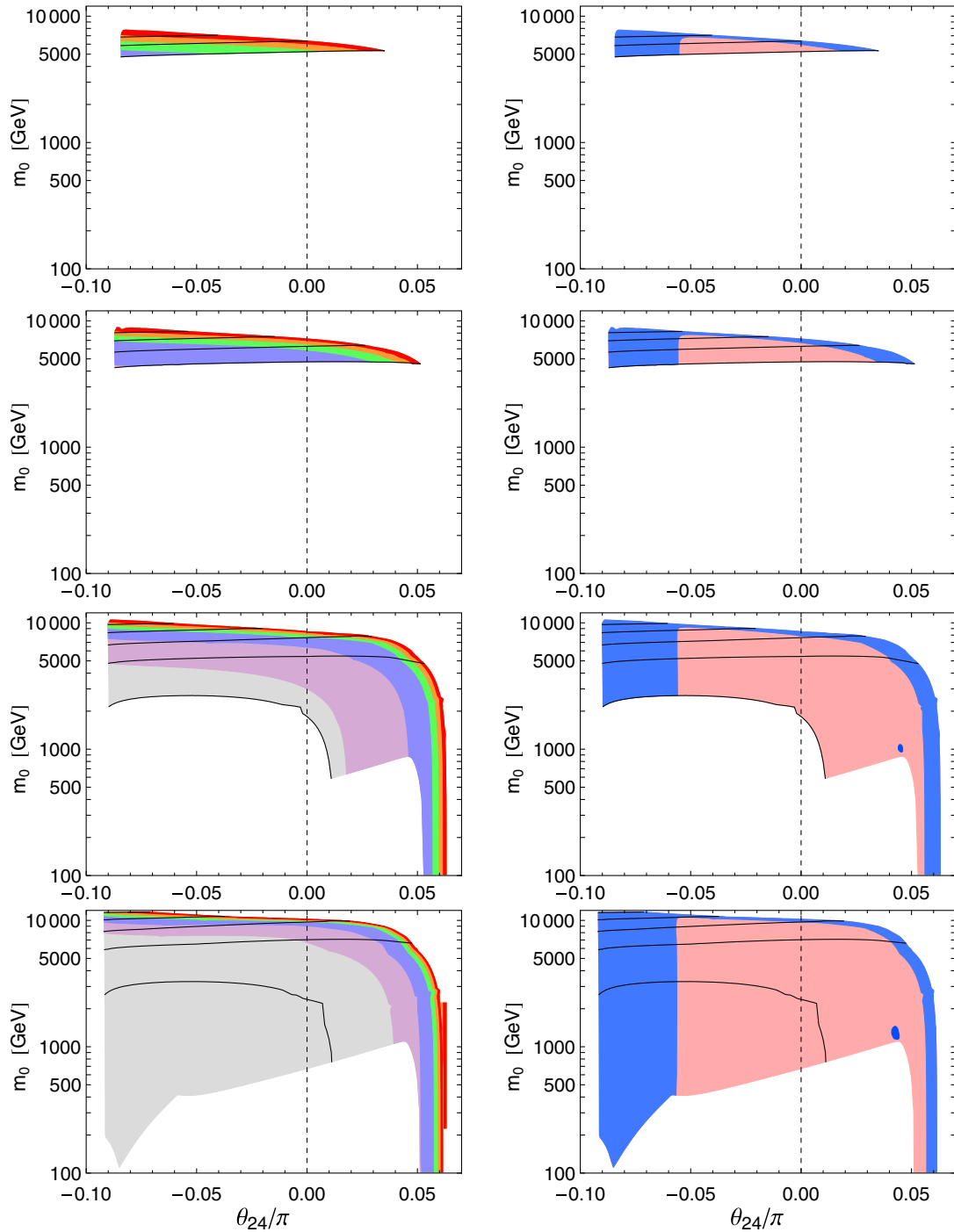


FIG. 2 (color online). Maps of the  $\mu$  parameter (left) and  $\Omega_{\text{DM}}h^2$  (right), as in Fig. 1, but with fixed  $M_3 = 1200, 1500, 2000,$  and  $2500$  GeV (from top to bottom) at  $M_U$ . In each case,  $\tan\beta = 10$ , and  $A_0 = 0$  at  $M_U$ . In the case of  $M_3 = 2500$  GeV, the lowest solid black line corresponds to a SuSpect prediction of  $M_h = 124$  GeV, while in the other cases it is  $M_h = 123$  GeV.

suppressed by the large ratio of gaugino masses to scalar masses yielding a nearly flavor-blind sfermion sector. Here the scalar squared masses are parametrized by the small flavor-preserving  $m_0^2$ , but in general they could be any similarly small scalar squared masses with arbitrary flavor structure without significantly affecting the results. In both the  $M_3 = 2000$  and  $2500$  GeV plots, the lower

boundary of the shaded allowed region is set by the imposed requirement that the LSP not be a charged stau. (If  $R$  parity is violated, this requirement could be relaxed.) Note that because of the requirement of accommodating  $M_h$ , the physical gluino mass has to be of order at least about 3 TeV, so that LHC discovery prospects may have to hinge on discovery of the lighter bino- and Higgsino-like

neutralino and chargino states instead. This will require very high luminosity because of the low cross section, and may be quite problematic.

In the  $M_3 = 2000$  and  $2500$  GeV plots of Fig. 2, there is also a small island of allowed neutralino dark matter visible centered near  $(\theta_{24}/\pi, m_0) = (0.043, 1300 \text{ GeV})$  in the latter plot, on the shores of which  $\Omega_{\text{DM}} h^2 = 0.12$ . Here the LSP is mostly binolike but with a significant mixing with somewhat heavier Higgsinos, and efficient annihilation of dark matter in the early universe crucially relies on the near-resonant coannihilation process through a charged Higgs scalar boson:  $\tilde{N}_1 \tilde{C}_1^\pm \rightarrow H^\pm \rightarrow tb$ , with an important role played also by neutral Higgs-mediated coannihilations  $\tilde{N}_1 \tilde{N}_{2,3} \rightarrow b\bar{b}$  mediated by neutral Higgs bosons  $A^0$  and  $H^0$ . The Higgsino-like  $\tilde{N}_2, \tilde{C}_1$  can be up to about 225 GeV heavier than the LSP here.

### III. MODELS WITH MODERATE STOP MIXING ( $A_0 = -m_0$ )

Next, consider models in which the usual CMSSM-like parameter  $A_0$  is constrained to be equal to  $-m_0$  at  $M_U$ . This provides for a stronger mixing of top squarks, which in turn increases the prediction for  $M_h$ , allowing for models to be viable with lower overall superpartner masses. The maps of  $\mu$  and  $\Omega_{\text{DM}} h^2$  in the  $m_0$  vs  $\theta_{24}/\pi$  plane are shown for four choices  $M_3 = 600, 1000, 1500,$  and  $2000$  GeV, in Fig. 3. Here I have fixed  $\tan\beta = 20$ . The color scheme is the same as in the previous figures.

Note that for  $A_0 = -m_0$ , this time there is no focus-point region with large  $m_0$  and small  $\mu$  that is consistent with the observed Higgs mass. (The focus point can be restored by generalizing it to include large nonuniversal scalar masses [27].) On the left side of the continent, there is again a region with allowed neutralino dark matter due to significant wino mixing in the LSP. However, this case is always associated with large  $|\mu|$  in these models, and so could be viewed as disfavored for seminatural supersymmetry and more generally in any motivational scheme in which  $|\mu|$  is taken to be a proxy for fine-tuning. In the  $M_3 = 1500$  and  $2000$  GeV cases, we again see islands (centered near  $\theta_{24}/\pi = 0.051$  and  $m_0 = 1300$  GeV in the latter case) of allowed neutralino dark matter associated with  $\tilde{N}_1 \tilde{C}_1^\pm \rightarrow tb$ , and  $\tilde{N}_1 \tilde{N}_{2,3} \rightarrow b\bar{b}$  coannihilations mediated by heavy Higgs bosons bringing about a reduction in the thermal relic abundance. These islands are significantly larger than in the  $A_0 = 0$  case of the previous section, but are again associated with  $\mu \gtrsim 1500$  GeV, with a mostly binolike LSP that is significantly mixed with Higgsinos that are up to 250 GeV heavier.

Although there is no region with small  $\mu$  or allowed neutralino dark matter in the CMSSM cases here (the vertical dashed lines in Fig. 3), the region with small  $\mu$  along the right side of the continent (with  $\theta_{24}/\pi \gtrsim 0.05$ ) persists, and in fact models with moderate and large  $m_0$  are viable for much smaller gaugino masses than in the case of

the previous section. This region extends down to very small  $m_0$  when  $M_3$  is larger than 1000 GeV at the grand unified theory scale, again corresponding to a gaugino mass dominated scenario in which flavor violation is naturally suppressed. The region can provide allowed neutralino dark matter due to the significant Higgsino content of the LSP, depending on how small  $\mu$  is. Note that in the case of  $M_3 = 2000$  GeV at  $M_U$ , the SuSpect prediction when  $m_0$  is small is for  $M_h$  between 124 and 125 GeV, which may, however, actually be too high in view of the three-loop radiative corrections [92,93,106,107]. For the  $M_3 = 1500$  GeV figure, the SuSpect prediction is between 123 and 124 GeV, and would therefore rely on three-loop or other radiative corrections not included in SuSpect in order to bring it to the observed range. Values of  $M_3$  between these two would interpolate between the two cases. As in Fig. 2, in  $M_3 = 1500$  and  $2000$  GeV in Fig. 3 the lower bound of the allowed shaded region, when it is not a solid black line, is where the stau would become the LSP.

### IV. MODELS WITH LARGER STOP MIXING ( $A_0 = -2m_0$ )

In this section, I consider models with larger stop mixing, by taking  $A_0 = -2m_0$  at  $M_U$ , so that  $M_h$  is made larger. In Fig. 5, I show the results of a map of this parameter space generalized to nonzero  $\theta_{24}$ , for  $\tan\beta = 10$ , varying  $m_0$  and four choices of  $M_3 = 600, 900, 1200,$  and  $1500$  GeV. Note that here we can accommodate the observed Higgs mass with much lower values of the gluino mass. The lowest value of 600 GeV was chosen because this gives a physical gluino mass of about  $M_{\tilde{g}} = 1400\text{--}1500$  GeV (depending on the other parameters), and lower values would likely be ruled out by direct searches at the LHC, although such searches specifically for this scenario have not been conducted. Recent searches for supersymmetry in the CMSSM case at ATLAS have used as a comparison model the case with  $\tan\beta = 30$  and  $A_0/m_0 = -2$  rather than 0. This allows the CMSSM models to accommodate  $M_h = 126$  GeV, unlike the old standard choices of  $\tan\beta = 10$  and  $A_0 = 0$ . A similar set of maps is therefore shown in Fig. 5 again for  $A_0/m_0 = -2$  but with  $\tan\beta = 30$ . For the CMSSM  $\theta_{24} = 0$  case, the ATLAS limit [1–3] is between  $M_3 = 550$  and 800 GeV, depending on  $m_0$ .

The maps shown in Figs. 4 and 5 only go up to  $M_3 = 1500$  and  $1200$  GeV respectively, to emphasize that this is all that is needed in order to accommodate the observed Higgs boson mass. However, there is nothing wrong with higher  $M_3$ , which would allow even lower  $m_0$ , and increase the regions where seminatural supersymmetry with small  $\mu$  is allowed. In fact, for  $M_3$  larger than about 1500 GeV, the results for small  $m_0$  are very similar to those of the previous sections, because then  $A_0$  will also be small compared to the overall scale set by gaugino masses,

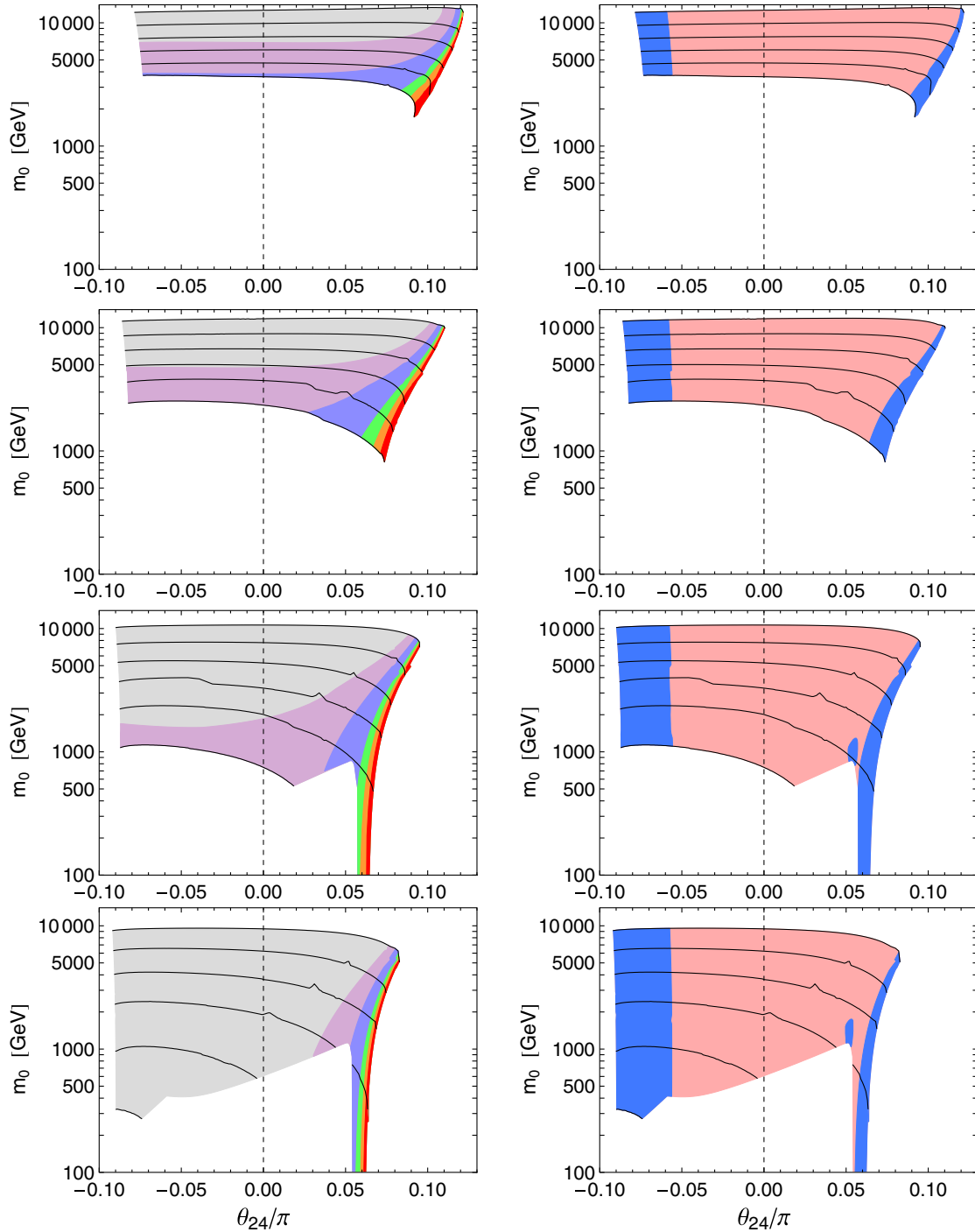


FIG. 3 (color online). Maps of the  $\mu$  parameter (left) and  $\Omega_{\text{DM}}h^2$  (right), as in Fig. 1, but with  $\tan\beta = 20$  and  $A_0 = -1$  and  $M_3 = 600, 1000, 1500,$  and  $2000$  GeV (from top to bottom) at  $M_U$ .

due to the assumed relation  $A_0 = -2m_0$ . Therefore, plots with larger  $M_3$  are not shown, for brevity. Note that the maps of Figs. 4 and 5 are also qualitatively similar to the  $A_0 = -m_0$  maps of the previous section, in many respects, even for the small  $M_3$  values shown. In particular, there is no focus-point region at large  $m_0$ , but there is a small  $\mu$  region for  $\theta_{24}/\pi = 0.055$  to  $0.08$ . The region is confined

to  $m_0 \lesssim 1200$  GeV here, because for larger  $A_0 = -2m_0$  the lighter top squark decreases in mass due to the top-squark mixing, and becomes the LSP. The thinner strips of allowed dark matter along the upper right-hand sides of the shaded allowed regions in Figs. 4 and 5 are stop coannihilation [135–138] and stop-mediated annihilation [34,36] regions, where the top squark is not much

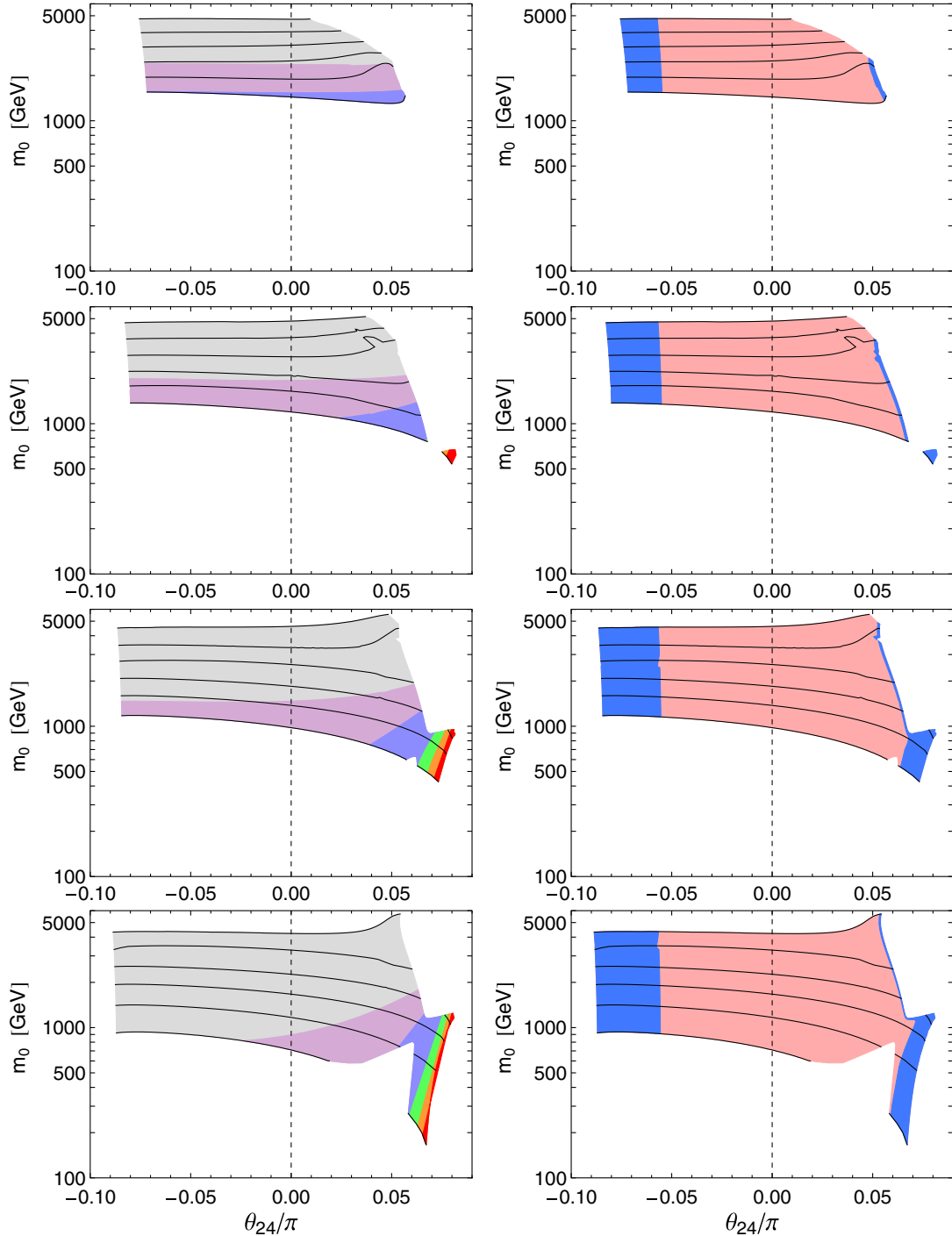


FIG. 4 (color online). Maps of the  $\mu$  parameter (left) and  $\Omega_{\text{DM}}h^2$  (right), as in Fig. 1, but with  $\tan\beta = 10$  and  $A_0 = -2m_0$  and  $M_3 = 600, 900, 1200,$  and  $1500$  GeV (from top to bottom) at  $M_U$ .

heavier than the LSP. The lower boundary wedges biting into the shaded allowed regions in Fig. 4 for  $M_3 = 1200$  and  $1500$  GeV are where the lighter stau is the LSP. In the  $M_3 = 900$  GeV case of Fig. 4, the regions vetoed by stop LSP and stau LSP collide, separating the small- $\mu$  region off into an island. The same thing is responsible for the islands in Fig. 5 for  $M_3 = 800, 1000,$  and  $1200$  GeV.

Throughout these islands, one finds  $\Omega_{\text{DM}}h^2 \lesssim 0.12$  due to a large Higgsino content of the LSP.

## V. SUPERPARTNER MASS SPECTRA AND DISCOVERY PROSPECTS

In this section, I will discuss the specifics of the superpartner mass spectrum for certain models discussed



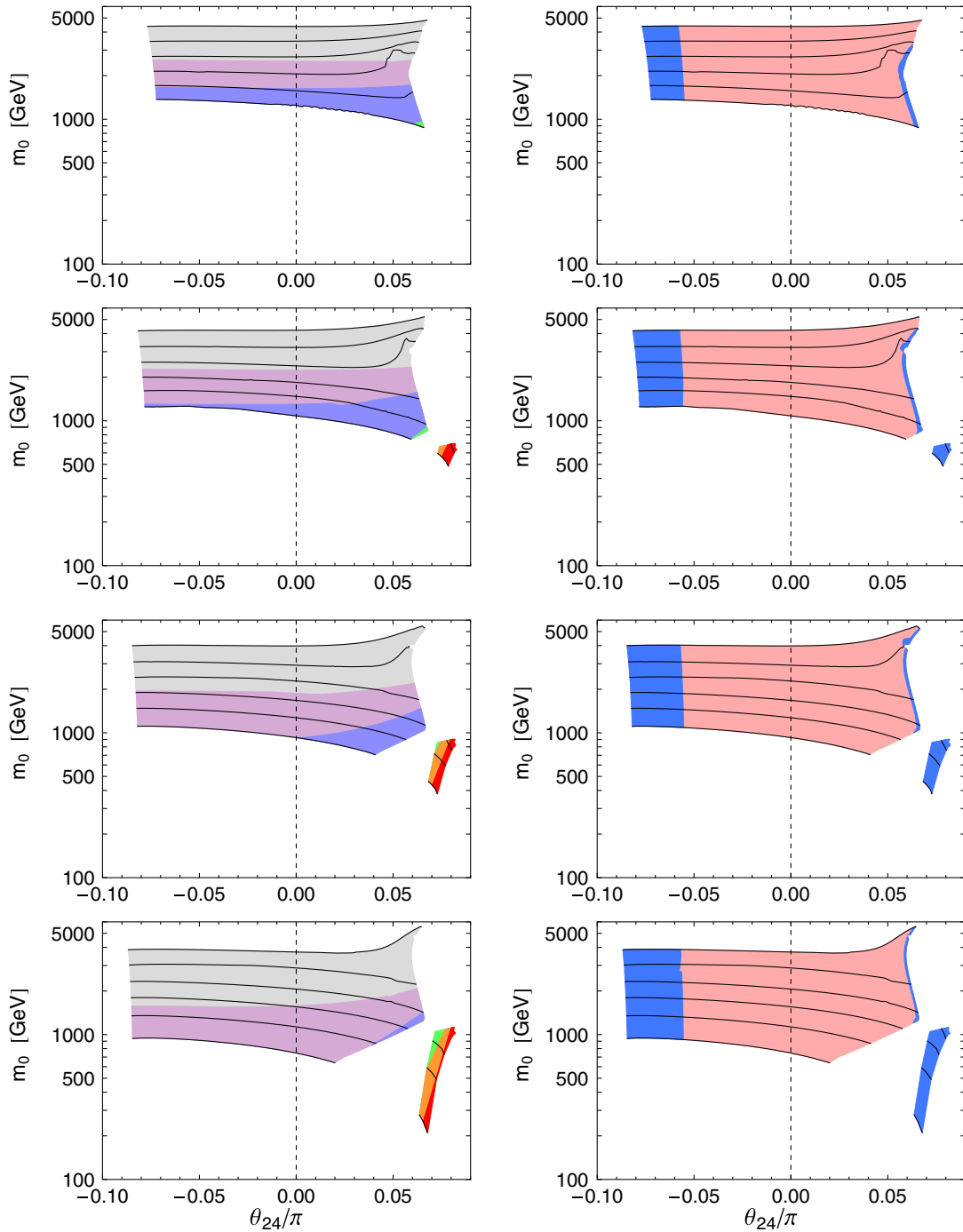


FIG. 5 (color online). Maps of the  $\mu$  parameter (left) and  $\Omega_{\text{DM}}h^2$  (right), as in Fig. 1, but with  $\tan\beta = 30$  and  $A_0 = -2m_0$  and  $M_3 = 600, 800, 1000,$  and  $1200$  GeV (from top to bottom) at  $M_U$ .

above. There are two distinct well-motivated branches of parameter space that I will consider. First, one can take seminaturalness as the main motivation, and require  $|\mu|$  less than a few hundred GeV. In this case, the predicted thermal  $\Omega_{\text{DM}}h^2$  is much less than 0.12, so then I will simply assume that axions (or some other particles) are the dark matter, and apply no constraints from direct detection. Second, one can require instead that

$\Omega_{\text{DM}}h^2 = 0.12$ , so that the neutralino LSP is the dark matter, with the correct thermal relic abundance. This requires larger values of  $\mu$ , but typically still in the range of about 1000 GeV. Here one can apply constraints from dark matter direct detection experiments.

In the first, “seminatural,” supersymmetry case, which is defined for practical purposes to include the region with  $\theta_{24} \gtrsim 0.05$  and small  $m_0^2$  at  $M_U$ , a typical one-parameter

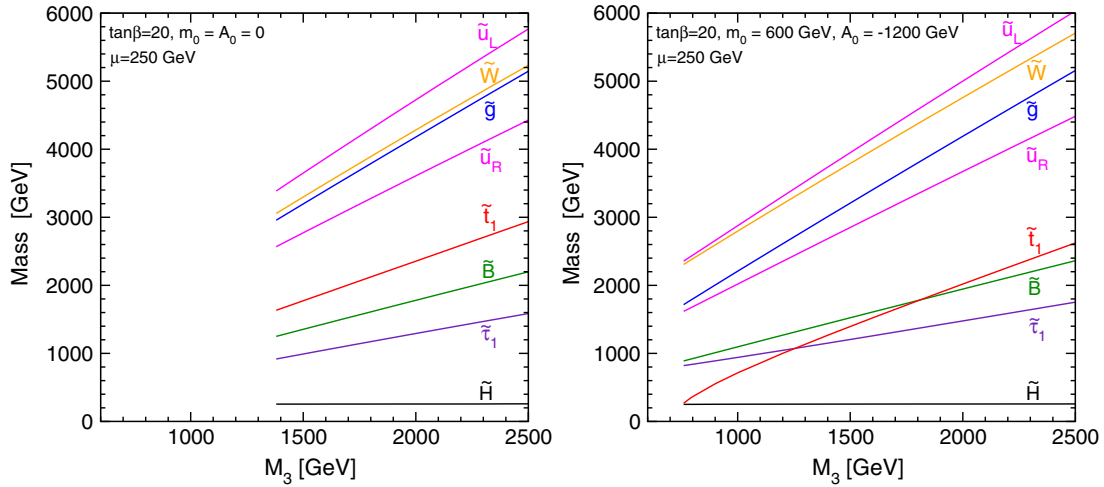


FIG. 6 (color online). Mass spectra for selected superpartners, as a function of  $M_3$  at  $M_U$ , for  $\tan\beta = 20$ , with  $m_0 = A_0 = 0$  (left panel) and  $m_0 = -A_0/2 = 600$  GeV (right panel). In each case, the gaugino mass nonuniversality parameter  $\theta_{24}$  is determined by requiring  $\mu = 250$  GeV. The lines labeled by  $\tilde{H}$  indicate the nearly degenerate  $\tilde{N}_1$ ,  $\tilde{C}_1$ , and  $\tilde{N}_2$ , while the lines labeled by  $\tilde{W}$  indicate the nearly degenerate  $\tilde{C}_2$ ,  $\tilde{N}_4$ , and  $\tilde{B}$  is  $\tilde{N}_3$ . Below the lower endpoints of the lines in the left panel, SuSpect predicts  $M_h < 123$  GeV. In the right panel, the lower endpoints are set by requiring that the LSP not be a top squark.

superpartner mass spectrum is shown in Fig. 6(a). Here I have taken  $\tan\beta = 20$  and  $m_0 = A_0 = 0$  GeV as in no-scale CMSSM models, and varied  $M_3$  at  $M_U$ , with the gaugino mass nonuniversality parameter  $\theta_{24}$  fixed for each model point so that  $\mu = 250$  GeV.

The left cutoff of the lines is fixed by demanding  $M_h > 123$  GeV according to SuSpect. The lightest superpartners are two mostly Higgsino-like neutralinos and a chargino, with masses given at tree level by the approximate formulas:

$$M_{\tilde{N}_1} = |\mu| - \frac{m_W^2[\pm 1 + \sin(2\beta)][M_1 + M_2 \tan^2\theta_W - \mu/\cos^2\theta_W]}{2(M_1 - \mu)(M_2 - \mu)} + \dots \quad (5.1)$$

$$M_{\tilde{C}_1} = |\mu| \mp \frac{m_W^2[\mu + M_2 \sin(2\beta)]}{M_2^2 - \mu^2} + \dots \quad (5.2)$$

$$M_{\tilde{N}_2} = |\mu| + \frac{m_W^2[\pm 1 - \sin(2\beta)][M_1 + M_2 \tan^2\theta_W + \mu/\cos^2\theta_W]}{2(M_1 + \mu)(M_2 + \mu)} + \dots \quad (5.3)$$

where electroweak symmetry breaking is treated as a perturbation, and  $\pm 1$  is the sign of  $\mu$ . The Higgsino-like states satisfy  $M_{\tilde{N}_1} < M_{\tilde{C}_1} < M_{\tilde{N}_2}$  for positive  $\mu$ , with a mass splitting that decreases as  $M_1$  and/or  $M_2$  are taken large compared to  $m_W$  and  $|\mu|$ . (In the specific model line shown, the total mass splitting of the Higgsino-like states,  $m_{\tilde{N}_2} - m_{\tilde{N}_1}$ , is a few GeV. One-loop radiative corrections to the tree-level formulas are significant, but can mostly be absorbed into the definition of the scale-dependent parameter  $\mu$ .) There is nothing special about the value of  $\mu = 250$  GeV chosen here; it could even be as low as the current bounds from LEP2 close to 100 GeV. The LHC discovery potential for this whole class of models is the same as discussed already in [20], and is extremely challenging. (See also [21]. A similar case with nearly degenerate

gauginos rather than Higgsinos is discussed in [139].) The direct production cross section for Higgsinos is quite small, and the decay products will give rise to soft leptons and jets, with significant physics and detector backgrounds and low trigger efficiencies, so that discovery may have to rely on extra radiated jets. Unlike the cases studied in [140,141], there are no superpartners that are close in mass that could decay to the Higgsinos; in particular, the very motivation of this class of seminatural supersymmetry models ensures that the winolike state masses will be around the gluino mass, and much too heavy to produce with an appreciable cross section at the LHC. From Fig. 6 we see that the discovery of the gluino and squarks is also quite problematic for the LHC, unless their masses are near the lower end of the range shown.

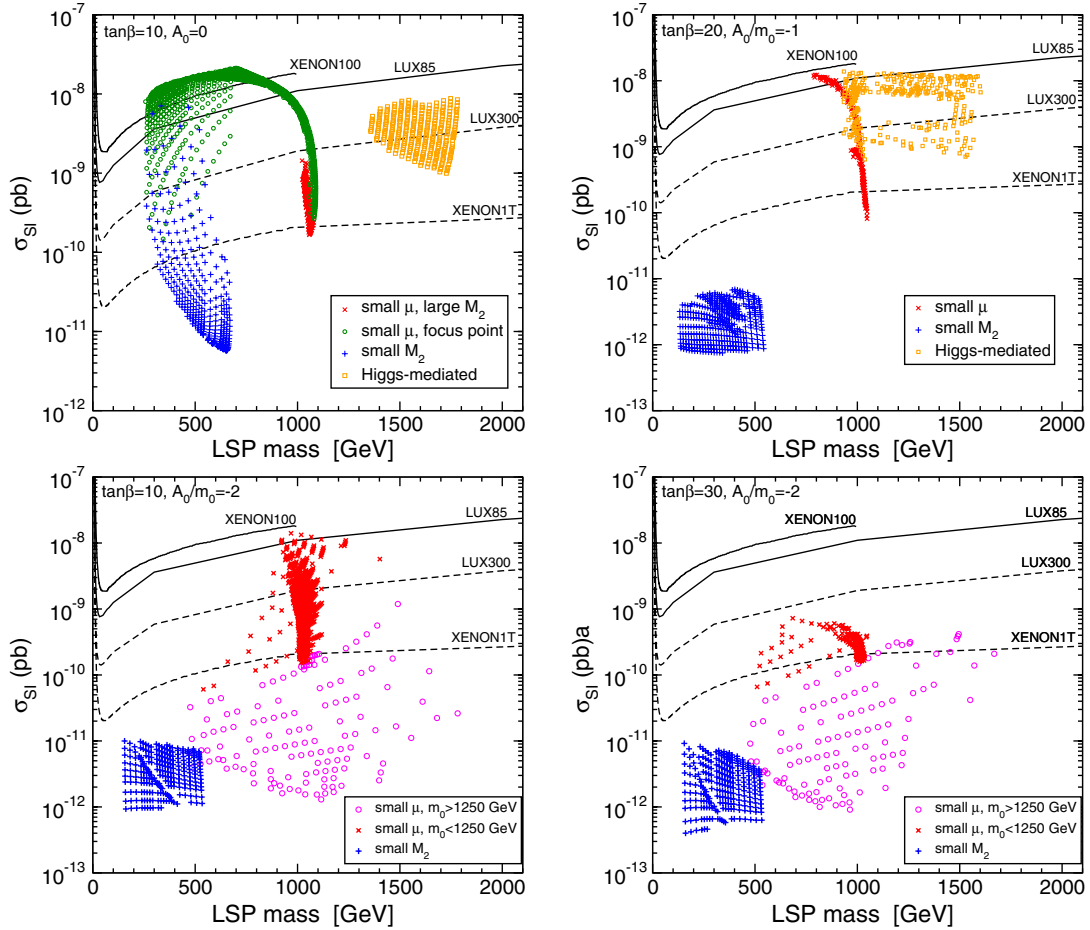


FIG. 7 (color online). The spin-independent LSP-nucleon cross section as a function of LSP mass, for models shown in Figs. 2, 3, 5, and 4 that satisfy  $\Omega_{\text{DM}} h^2 = 0.120 \pm 0.005$ . The model point symbols are coded according to four regions: the small- $\mu$  region with large  $M_2$  at positive  $\theta_{24}$ ; the focus-point region with small  $\mu$  and  $m_0 > 5000$  GeV, which occurs only in the first panel; the small  $M_2$  region with negative  $\theta_{24}$ ; and the Higgs-mediated coannihilation island region, which occurs only in the top two panels. In the bottom two panels, the small- $\mu$  region points with  $m_0$  greater than 1250 GeV are shown separately (circles).

It may also be possible to search for the light Higgsino-like states using weak boson fusion [142–144].

A more optimistic model line is shown in Fig. 6(b), where now I have chosen  $m_0 = 600$  GeV and  $A_0 = -1200$  GeV in order to accommodate  $M_h$  consistently with lower superpartner masses. Again I have fixed  $\tan\beta = 20$  and adjusted  $\theta_{24}$  for each model point so that  $\mu = 250$  GeV, providing for light Higgsino-like states. In this case, the lower endpoint of the model line is given by the point at which a top squark becomes the LSP, and in this case the gluino and right-handed squarks could perhaps already be light enough to detect with the current data at the LHC with  $\sqrt{s} = 8$  TeV.

In both of the above cases, the heavier Higgsino-like states will decay through off-shell weak bosons to the LSP according to

$$\tilde{C}_1 \rightarrow W^{(*)} \tilde{N}_1, \quad \tilde{N}_2 \rightarrow Z^{(*)} \tilde{N}_1, \quad (5.4)$$

with branching ratios that are distorted by kinematics to disfavor tau and charm final states, to an extent that

depends on the mass differences. The lighter top squark will decay according to

$$\tilde{t}_1 \rightarrow \begin{cases} b\tilde{C}_1 & (\sim 50\%), \\ t\tilde{N}_2 & (\sim 25\%), \\ t\tilde{N}_1 & (\sim 25\%), \end{cases} \quad (5.5)$$

for  $m_{\tilde{t}_1} - m_{\tilde{N}_1} \gg m_t$ , and

$$\tilde{t}_1 \rightarrow b\tilde{C}_1 \quad (100\%) \quad (5.6)$$

for  $m_{\tilde{t}_1} - m_{\tilde{N}_1} < m_t$ , and branching ratios that are intermediate between these extremes if  $m_{\tilde{t}_1} - m_{\tilde{N}_1}$  is comparable to but larger than  $m_t$ . The lighter up and down quarks decay according to  $\tilde{q}_R \rightarrow q\tilde{N}_3$  with a nearly 100% branching ratio, while the gluino has its largest decay branching fractions equally to  $\tilde{t}_1$  and  $\tilde{t}_1$ . The binolike neutralino  $\tilde{N}_3$  also has large branching fractions to  $\tilde{t}_1$  and  $\tilde{t}_1$ , but also to

$W^\pm \tilde{C}_1^\mp$ . Thus the usual supersymmetry signals apply for gluino and squark production, but only if they are light enough to be produced in sufficient numbers at the LHC. Note that the winolike states  $\tilde{C}_2, \tilde{N}_4$  are heavier than the gluino and so will not participate in LHC discovery signals.

Finally, I turn to the dark matter motivated alternative in which one requires a thermal relic abundance in accord with the WMAP and Planck observations. This requires a larger value of  $|\mu|/M_1$  in order to avoid overly efficient annihilation of the dark matter, so the superpartner mass spectrum looks qualitatively similar to Fig. 6, except that the Higgsino-like states will be much heavier, of order 1000 GeV. I show in the first panel of Fig. 7 the predictions for the spin-independent LSP-nucleon cross sections (obtained from version 3.1 of micrOmegas [111–114] with the default choices for nuclear matrix elements, including  $f_s = 0.0447$ ) for the models of Fig. 2 with  $\tan\beta = 10$ , varying  $\theta_{24}$  and  $m_0$ , and  $M_3$  continuously varied from 1200 to 2500 GeV. Here, by varying  $\theta_{24}$ , I require that the thermal relic abundance lies in the range  $\Omega_{\text{DM}} h^2 = 0.120 \pm 0.005$ . The model point symbols are coded according to four regions: the small- $\mu$  region with large  $M_2$  and  $\theta_{24}/\pi > 0.05$  (red); the focus-point region with small  $\mu$  and  $m_0 > 5000$  GeV (green); the small  $M_2$  region with  $\theta_{24}/\pi \lesssim -0.055$  (blue); and the Higgs-mediated coannihilation island region (orange). The boundaries between the first and second regions and the second and third regions are fuzzy, as indicated by the overlap of model points. Also shown are the present limits from XENON100 [119] and the LUX 85 day data [120] (solid lines), and some projected reaches for LUX 300 day [145] and XENON 1 T [146] runs (dashed lines). Some, but not all, of the focus-point models are in tension with the XENON100 and LUX85 limits. (Here it is good to keep in mind the significant uncertainties associated with nuclear matrix elements.) However, the other regions are clearly safely beyond the current limits. Most of the small- $\mu$  region and the Higgs-mediated island will eventually be explored by ton-class direct detection experiments, but the bino-wino coannihilation region will continue to be a challenge.

Similarly, the remaining three panels of Fig. 7 show the corresponding spin-independent LSP-nucleon cross sections for the other three cases that were studied above in Figs. 3, 5, and 4. These cases do not have focus-point regions, but are otherwise qualitatively similar to the first panel. In the cases of  $A_0 = -2m_0$ , the regions with small  $\mu$  that have  $m_0 > 1250$  GeV are indicated separately, and mostly consist of models where the dark matter thermal abundance arises in part due to coannihilations with top squarks. We see that the region with relatively small  $\mu$  will be nearly, but not completely, probed by ton-class direct

dark matter detection experiments, provided that  $m_0$  is not larger than roughly 1250 GeV, depending on the other parameters of the model. For the larger  $m_0$  case with stop coannihilation, and for the wino-coannihilation case, it will remain very challenging for direct detection experiments to probe the models for some time.

## VI. OUTLOOK

The discovery of the Higgs boson with a mass near 126 GeV is consistent with supersymmetry, and provides an important clue as to the superpartner mass spectrum.<sup>1</sup> This clue fits nicely with an expectation that the top squarks should be heavy. A heavy spectrum of squark and slepton masses also fits well with the current nonobservation of squarks and the gluino at the LHC, and the suppression of flavor violation that one might otherwise expect in supersymmetry. However, it is in tension with expectations from naturalness. In this paper I have embraced the idea of only requiring seminatural supersymmetry, where  $|\mu|$  is required to be of order a few hundred GeV or less, but no expectations are taken with regard to other superpartner masses.

Within the framework of nonuniversal gaugino masses at the scale of gauge coupling unification, this is seen to be nicely consistent with the idea of flavor-preserving sfermion masses coming from gaugino mass dominance,  $m_{1/2}^2 \gg m_0^2, A_0^2$ , like the well-known no-scale or “gaugino mediation” ideas. Although this idea was only mapped out in this paper for a tiny subset of possible models, it should be clear that this will work much more generally. For example, one can see from Fig. 1 that the same thing can occur for  $\theta_{24}/\pi \approx 0.33$ , a region of parameter space that is far from the CMSSM case. The region of parameter space that we may be lead to through the clues mentioned above can be quite challenging both for the future explorations of the LHC and for direct dark matter experiments.

## ACKNOWLEDGMENTS

I thank Graham Kribs and James Younkin for relevant conversations. This work was supported in part by the National Science Foundation Grant No. PHY-1068369. This research was supported in part by the National Science Foundation under Grant No. NSF PHY11-25915.

<sup>1</sup>It is interesting that for any given model framework, the usefulness of this clue is already limited by the theoretical uncertainties in the Higgs mass computation, which one can hope will be reduced with further work.



- [1] G. Aad *et al.* (ATLAS Collaboration), Report No. ATLAS-CONF-2013-047, 2013.
- [2] G. Aad *et al.* (ATLAS Collaboration), Report No. ATLAS-CONF-2013-062, 2013.
- [3] G. Aad *et al.* (ATLAS Collaboration), arXiv:1308.1841.
- [4] S. Chatrchyan *et al.* (CMS Collaboration), Report No. CMS-PAS-SUS-13-012.
- [5] D. S. M. Alves, E. Izaguirre, and J. G. Wacker, *Phys. Lett. B* **702**, 64 (2011).
- [6] D. S. M. Alves, E. Izaguirre, and J. G. Wacker, *J. High Energy Phys.* **10** (2011) 012.
- [7] T. J. LeCompte and S. P. Martin, *Phys. Rev. D* **84**, 015004 (2011).
- [8] T. J. LeCompte and S. P. Martin, *Phys. Rev. D* **85**, 035023 (2012).
- [9] H. Baer, V. Barger, P. Huang, A. Mustafayev, and X. Tata, *Phys. Rev. Lett.* **109**, 161802 (2012).
- [10] J. L. Feng, *Annu. Rev. Nucl. Part. Sci.* **63**, 351 (2013).
- [11] N. Craig, arXiv:1309.0528.
- [12] H. Baer, V. Barger, and D. Mickelson, *Phys. Rev. D* **88**, 095013 (2013).
- [13] J. E. Kim and H. P. Nilles, *Phys. Lett.* **138B**, 150 (1984).
- [14] G. F. Giudice and A. Masiero, *Phys. Lett. B* **206**, 480 (1988).
- [15] U. Ellwanger, C. Hugonie, and A. M. Teixeira, *Phys. Rep.* **496**, 1 (2010).
- [16] M. Papucci, J. T. Ruderman, and A. Weiler, *J. High Energy Phys.* **09** (2012) 035.
- [17] J. A. Evans, Y. Kats, D. Shih, and M. J. Strassler, arXiv:1310.5758.
- [18] G. L. Kane and J. D. Wells, *Phys. Rev. Lett.* **76**, 4458 (1996).
- [19] G. L. Kane, in *Perspectives on Supersymmetry*, edited by G. L. Kane (World Scientific, Singapore, 2010), pp. 352–354.
- [20] H. Baer, V. Barger, and P. Huang, *J. High Energy Phys.* **11** (2011) 031.
- [21] C. Han, A. Kobakhidze, N. Liu, A. Saavedra, L. Wu, and J. M. Yang, arXiv:1310.4274.
- [22] K. L. Chan, U. Chattopadhyay, and P. Nath, *Phys. Rev. D* **58**, 096004 (1998).
- [23] J. L. Feng, K. T. Matchev, and T. Moroi, *Phys. Rev. Lett.* **84**, 2322 (2000).
- [24] J. L. Feng, K. T. Matchev, and T. Moroi, *Phys. Rev. D* **61**, 075005 (2000).
- [25] J. L. Feng, K. T. Matchev, and F. Wilczek, *Phys. Lett. B* **482**, 388 (2000).
- [26] J. L. Feng, K. T. Matchev, and D. Sanford, *Phys. Rev. D* **85**, 075007 (2012).
- [27] J. L. Feng and D. Sanford, *Phys. Rev. D* **86**, 055015 (2012).
- [28] G. L. Kane and S. F. King, *Phys. Lett. B* **451**, 113 (1999).
- [29] M. Bastero-Gil, G. L. Kane, and S. F. King, *Phys. Lett. B* **474**, 103 (2000).
- [30] K. Huitu, J. Laamanen, P. N. Pandita, and S. Roy, *Phys. Rev. D* **72**, 055013 (2005).
- [31] H. Baer, A. Mustafayev, E.-K. Park, S. Profumo, and X. Tata, *J. High Energy Phys.* **04** (2006) 041.
- [32] K. Huitu, J. Laamanen, P. N. Pandita, and S. Roy, *Pramana* **69**, 823 (2007).
- [33] H. Abe, T. Kobayashi, and Y. Omura, *Phys. Rev. D* **76**, 015002 (2007).
- [34] S. P. Martin, *Phys. Rev. D* **75**, 115005 (2007).
- [35] B. Ananthanarayan and P. N. Pandita, *Int. J. Mod. Phys. A* **22**, 3229 (2007).
- [36] S. P. Martin, *Phys. Rev. D* **76**, 095005 (2007).
- [37] S. F. King, J. P. Roberts, and D. P. Roy, *J. High Energy Phys.* **10** (2007) 106.
- [38] H. Baer, A. Mustafayev, H. Summy, and X. Tata, *J. High Energy Phys.* **10** (2007) 088.
- [39] D. Horton and G. G. Ross, *Nucl. Phys.* **B830**, 221 (2010).
- [40] N. Okada, S. Raza, and Q. Shafi, *Phys. Rev. D* **84**, 095018 (2011).
- [41] J. E. Younkin and S. P. Martin, *Phys. Rev. D* **85**, 055028 (2012).
- [42] F. Brummer and W. Buchmuller, *J. High Energy Phys.* **05** (2012) 006.
- [43] S. Caron, J. Laamanen, I. Niessen, and A. Strubig, *J. High Energy Phys.* **06** (2012) 008.
- [44] S. Antusch, L. Calibbi, V. Maurer, M. Monaco, and M. Spinrath, *J. High Energy Phys.* **01** (2013) 187.
- [45] I. Gogoladze, F. Nasir, and Q. Shafi, *Int. J. Mod. Phys. A* **28**, 1350046 (2013).
- [46] A. Spies and G. Anton, *J. Cosmol. Astropart. Phys.* **06** (2013) 022.
- [47] I. Gogoladze, F. Nasir, and Q. Shafi, arXiv:1306.5699.
- [48] T. T. Yanagida and N. Yokozaki, *Phys. Lett. B* **722**, 355 (2013).
- [49] D. J. Miller and A. P. Morais, arXiv:1307.1373.
- [50] M. A. Ajaib, I. Gogoladze, and Q. Shafi, arXiv:1307.4882.
- [51] M. Badziak, M. Olechowski, and S. Pokorski, arXiv:1307.7999.
- [52] T. T. Yanagida and N. Yokozaki, *J. High Energy Phys.* **11** (2013) 020.
- [53] A. Kaminska, G. G. Ross, and K. Schmidt-Hoberg, *J. High Energy Phys.* **11** (2013) 209.
- [54] M. E. Cabrera, A. Casas, R. R. de Austri, and G. Bertone, arXiv:1311.7152.
- [55] J. R. Ellis, C. Kounnas, and D. V. Nanopoulos, *Nucl. Phys.* **B247**, 373 (1984).
- [56] J. R. Ellis, K. Enqvist, D. V. Nanopoulos, and K. Tamvakis, *Phys. Lett.* **155B**, 381 (1985).
- [57] M. Drees, *Phys. Lett.* **158B**, 409 (1985).
- [58] G. Anderson, C. H. Chen, J. F. Gunion, J. D. Lykken, T. Moroi, and Y. Yamada, arXiv:hep-ph/9609457.
- [59] G. Anderson, H. Baer, C. h. Chen, and X. Tata, *Phys. Rev. D* **61**, 095005 (2000).
- [60] J. Chakraborty and A. Raychaudhuri, *Phys. Lett. B* **673**, 57 (2009).
- [61] S. P. Martin, *Phys. Rev. D* **79**, 095019 (2009).
- [62] G. Aad *et al.* (ATLAS Collaboration), *Phys. Lett. B* **716**, 1 (2012).
- [63] S. Chatrchyan *et al.* (CMS Collaboration), *Phys. Lett. B* **716**, 30 (2012).
- [64] G. Aad *et al.* (ATLAS Collaboration), Report No. ATLAS-CONF-2013-014, 2013.
- [65] S. Chatrchyan *et al.* (CMS Collaboration), Report No. CMS-PAS-HIG-12-045, 2012.
- [66] J. R. Ellis, G. Ridolfi, and F. Zwirner, *Phys. Lett. B* **257**, 83 (1991).
- [67] Y. Okada, M. Yamaguchi, and T. Yanagida, *Prog. Theor. Phys.* **85**, 1 (1991).

- [68] H. E. Haber and R. Hempfling, *Phys. Rev. Lett.* **66**, 1815 (1991).
- [69] A. Brignole, *Phys. Lett. B* **281**, 284 (1992).
- [70] P. H. Chankowski, S. Pokorski, and J. Rosiek, *Phys. Lett. B* **286**, 307 (1992).
- [71] P. H. Chankowski, S. Pokorski, and J. Rosiek, *Nucl. Phys.* **B423**, 437 (1994).
- [72] R. Hempfling and A. H. Hoang, *Phys. Lett. B* **331**, 99 (1994).
- [73] J. A. Casas, J. R. Espinosa, M. Quiros, and A. Riotto, *Nucl. Phys.* **B436**, 3 (1995); **B439**, 466(E) (1995).
- [74] A. Dabelstein, *Z. Phys. C* **67**, 495 (1995).
- [75] M. S. Carena, J. R. Espinosa, M. Quiros, and C. E. M. Wagner, *Phys. Lett. B* **355**, 209 (1995).
- [76] M. S. Carena, M. Quiros, and C. E. M. Wagner, *Nucl. Phys.* **B461**, 407 (1996).
- [77] S. Heinemeyer, W. Hollik, and G. Weiglein, *Phys. Rev. D* **58**, 091701 (1998).
- [78] S. Heinemeyer, W. Hollik, and G. Weiglein, *Phys. Lett. B* **440**, 296 (1998).
- [79] R.-J. Zhang, *Phys. Lett. B* **447**, 89 (1999).
- [80] J. R. Espinosa and R.-J. Zhang, *J. High Energy Phys.* **03** (2000) 026.
- [81] M. S. Carena, H. E. Haber, S. Heinemeyer, W. Hollik, C. E. M. Wagner, and G. Weiglein, *Nucl. Phys.* **B580**, 29 (2000).
- [82] J. R. Espinosa and R.-J. Zhang, *Nucl. Phys.* **B586**, 3 (2000).
- [83] G. Degrassi, P. Slavich, and F. Zwirner, *Nucl. Phys.* **B611**, 403 (2001).
- [84] A. Brignole, G. Degrassi, P. Slavich, and F. Zwirner, *Nucl. Phys.* **B631**, 195 (2002).
- [85] A. Brignole, G. Degrassi, P. Slavich, and F. Zwirner, *Nucl. Phys.* **B643**, 79 (2002).
- [86] S. P. Martin, *Phys. Rev. D* **65**, 116003 (2002).
- [87] S. P. Martin, *Phys. Rev. D* **66**, 096001 (2002).
- [88] S. P. Martin, *Phys. Rev. D* **67**, 095012 (2003).
- [89] S. P. Martin, *Phys. Rev. D* **68**, 075002 (2003).
- [90] S. P. Martin, *Phys. Rev. D* **71**, 016012 (2005).
- [91] S. P. Martin and D. G. Robertson, *Comput. Phys. Commun.* **174**, 133 (2006).
- [92] Stephen P. Martin, *Phys. Rev. D* **75**, 055005 (2007).
- [93] R. V. Harlander, P. Kant, L. Mihaila, and M. Steinhauser, *Phys. Rev. Lett.* **100**, 191602 (2008).
- [94] S. Heinemeyer, W. Hollik, and G. Weiglein, *Comput. Phys. Commun.* **124**, 76 (2000).
- [95] S. Heinemeyer, W. Hollik, and G. Weiglein, *Eur. Phys. J. C* **9**, 343 (1999).
- [96] G. Degrassi, S. Heinemeyer, W. Hollik, P. Slavich, and G. Weiglein, *Eur. Phys. J. C* **28**, 133 (2003).
- [97] M. Frank, T. Hahn, S. Heinemeyer, W. Hollik, H. Rzehak, and G. Weiglein, *J. High Energy Phys.* **02** (2007) 047.
- [98] T. Hahn, S. Heinemeyer, W. Hollik, H. Rzehak, and G. Weiglein, *Comput. Phys. Commun.* **180**, 1426 (2009).
- [99] B. C. Allanach, *Comput. Phys. Commun.* **143**, 305 (2002).
- [100] A. Djouadi, J. L. Kneur, and G. Moultaka, *Comput. Phys. Commun.* **176**, 426 (2007).
- [101] W. Porod, *Comput. Phys. Commun.* **153**, 275 (2003).
- [102] J. S. Lee, A. Pilaftsis, M. S. Carena, S. Y. Choi, M. Drees, J. R. Ellis, and C. E. M. Wagner, *Comput. Phys. Commun.* **156**, 283 (2004).
- [103] J. S. Lee, M. Carena, J. Ellis, A. Pilaftsis, and C. E. M. Wagner, *Comput. Phys. Commun.* **180**, 312 (2009).
- [104] J. S. Lee, M. Carena, J. Ellis, A. Pilaftsis, and C. E. M. Wagner, *Comput. Phys. Commun.* **184**, 1220 (2013).
- [105] F. E. Paige, S. D. Protopopescu, H. Baer, and X. Tata, *arXiv:hep-ph/0312045*.
- [106] P. Kant, R. V. Harlander, L. Mihaila, and M. Steinhauser, *J. High Energy Phys.* **08** (2010) 104.
- [107] J. L. Feng, P. Kant, S. Profumo, and D. Sanford, *arXiv:1306.2318*.
- [108] C. F. Berger, J. S. Gainer, J. L. Hewett, and T. G. Rizzo, *J. High Energy Phys.* **02** (2009) 023.
- [109] M. W. Cahill-Rowley, J. L. Hewett, A. Ismail, and T. G. Rizzo, *Phys. Rev. D* **86**, 075015 (2012).
- [110] M. Cahill-Rowley, J. L. Hewett, A. Ismail, and T. G. Rizzo, *arXiv:1307.8444*.
- [111] G. Belanger, F. Boudjema, A. Pukhov, and A. Semenov, *Comput. Phys. Commun.* **180**, 747 (2009).
- [112] G. Belanger, F. Boudjema, A. Pukhov, and A. Semenov, *Comput. Phys. Commun.* **176**, 367 (2007).
- [113] G. Belanger, F. Boudjema, A. Pukhov, and A. Semenov, *Comput. Phys. Commun.* **174**, 577 (2006).
- [114] G. Belanger, F. Boudjema, A. Pukhov, and A. Semenov, *Comput. Phys. Commun.* **149**, 103 (2002).
- [115] L. Covi, J. E. Kim, and L. Roszkowski, *Phys. Rev. Lett.* **82**, 4180 (1999).
- [116] L. Covi, H.-B. Kim, J. E. Kim, and L. Roszkowski, *J. High Energy Phys.* **05** (2001) 033.
- [117] J. L. Feng, A. Rajaraman, and F. Takayama, *Phys. Rev. Lett.* **91**, 011302 (2003).
- [118] K.-Y. Choi, L. Covi, J. E. Kim, and L. Roszkowski, *J. High Energy Phys.* **04** (2012) 106.
- [119] E. Aprile *et al.* (XENON100 Collaboration), *Phys. Rev. Lett.* **109**, 181301 (2012).
- [120] D. S. Akerib *et al.* (LUX Collaboration), *arXiv:1310.8214*.
- [121] C. L. Bennett *et al.* (WMAP Collaboration), *Astrophys. J. Suppl. Ser.* **208**, 20 (2013).
- [122] P. A. R. Ade *et al.* (Planck Collaboration), *arXiv:1303.5076*.
- [123] E. Cremmer, S. Ferrara, C. Kounnas, and D. V. Nanopoulos, *Phys. Lett.* **133B**, 61 (1983).
- [124] J. R. Ellis, C. Kounnas, and D. V. Nanopoulos, *Nucl. Phys.* **B247**, 373 (1984).
- [125] A. B. Lahanas and D. V. Nanopoulos, *Phys. Rep.* **145**, 1 (1987).
- [126] K. Inoue, M. Kawasaki, M. Yamaguchi, and T. Yanagida, *Phys. Rev. D* **45**, 328 (1992).
- [127] D. E. Kaplan, G. D. Kribs, and M. Schmaltz, *Phys. Rev. D* **62**, 035010 (2000).
- [128] Z. Chacko, M. A. Luty, A. E. Nelson, and E. Ponton, *J. High Energy Phys.* **01** (2000) 003.
- [129] A. Birkedal-Hansen and B. D. Nelson, *Phys. Rev. D* **64**, 015008 (2001).
- [130] H. Baer, A. Mustafayev, E.-K. Park, and S. Profumo, *J. High Energy Phys.* **07** (2005) 046.
- [131] H. Baer, T. Krupovnickas, A. Mustafayev, E.-K. Park, S. Profumo, and X. Tata, *J. High Energy Phys.* **12** (2005) 011.
- [132] M. Ibe, A. Kamada, and S. Matsumoto, *arXiv:1311.2162*.
- [133] N. Arkani-Hamed, A. Delgado, and G. F. Giudice, *Nucl. Phys.* **B741**, 108 (2006).

- [134] M. Drees and M. M. Nojiri, *Phys. Rev. D* **47**, 376 (1993).
- [135] M. E. Gomez, G. Lazarides, and C. Pallis, *Phys. Rev. D* **61**, 123512 (2000).
- [136] C. Boehm, A. Djouadi, and M. Drees, *Phys. Rev. D* **62**, 035012 (2000).
- [137] J. R. Ellis, K. A. Olive, and Y. Santoso, *Astropart. Phys.* **18**, 395 (2003).
- [138] C. Balazs, M. Carena, and C. E. M. Wagner, *Phys. Rev. D* **70**, 015007 (2004).
- [139] S. Gori, S. Jung, and L.-T. Wang, [arXiv:1307.5952](https://arxiv.org/abs/1307.5952).
- [140] H. Baer, V. Barger, P. Huang, D. Mickelson, A. Mustafayev, W. Sreethawong, and X. Tata, *Phys. Rev. Lett.* **110**, 151801 (2013).
- [141] T. Han, S. Padhi, and S. Su, *Phys. Rev. D* **88**, 115010 (2013).
- [142] G. F. Giudice, T. Han, K. Wang, and L.-T. Wang, *Phys. Rev. D* **81**, 115011 (2010).
- [143] B. Dutta, A. Gurrola, W. Johns, T. Kamon, P. Sheldon, and K. Sinha, *Phys. Rev. D* **87**, 035029 (2013).
- [144] A. G. Delannoy, B. Dutta, A. Gurrola, W. Johns, T. Kamon, E. Luiggi, A. Melo, P. Sheldon *et al.*, *Phys. Rev. Lett.* **111**, 061801 (2013).
- [145] D. McKinsey and R. Gaitskell (for the LUX Collaboration), at Sanford Underground Research Facility, 2013 (unpublished).
- [146] K. Arisaka (for the XENON Collaboration), in Snowmass on the Mississippi (CSS 2013), 2013 (unpublished).